ChemComm

Photo-stable and highly emissive glassy organic dots exhibiting thermally activated delayed fluorescence

Journal:	*ChemComm*
Manuscript ID	CC-COM-02-2019-001420.R1
Article Type:	Communication

ChemComm

Communication

Photo-stable and highly emissive glassy organic dots exhibiting thermally activated delayed fluorescence

Youichi Tsuchiya,*[a,b] Koudai Ikesue,[a,b,c] Hajime Nakanotani,[a,b,c] and Chihaya Adachi*[a,b,c,d]

Received 00th January 20xx,
Accepted 00th January 20xx

DOI: 10.1039/x0xx00000x

www.rsc.org/

Organic nanoparticles (O-dots) with a high photoluminescence quantum yield (94%) and long-lived delayed emission (3.1 μs) originating from thermally activated delayed fluorescence (TADF) were developed as glassy state particles through the oil in water emulsion under high pressure (<20 bar). The TADF glassy O-dots exhibit not only good dispersibility and high photo-stability in water but also good uptake properties into living cells. The glassy O-dots will open new uses for organic emitter in biological applications.

In biology and biochemistry research, light-emitting materials play very important roles, most prominently as exogenous probes for imaging or sensing. For example, phosphorescent materials have been used to probe for oxygen based on the suppression of emission by energy transfer from the emitters to oxygen.[1] Lanthanide complexes having long-lived emission can act as imaging probes in time-resolved fluorescence microscopy (TRFM) imaging,[2] which allows imaging without interference from autofluorescence of biomaterials.[3] Quantum dots (Q-dots) exhibiting narrow emission spectra and high photoluminescence quantum yields (Φ_{PL}) are promising for multi-staining imaging.[4,5] Recently, the discovery of emitters having aggregation-induced enhanced emission (AIEE) properties has allowed the bio-imaging application of water-insoluble organic emitters by O-dots.[6]

[a] *Center for Organic Photonics and Electronics Research (OPERA), Kyushu University, 744 Motooka, Nishi-ku, Fukuoka 819-0395, Japan. E-mail: tsuchiya@opera.kyushu-u.ac.jp, nakanotani@ cstf.kyushu-u.ac.jp, adachi@cstf.kyushu-u.ac.jp*
[b] *JST, ERATO, Adachi Molecular Exciton Engineering Project, Kyushu University, 744 Motooka, Nishi-ku, Fukuoka 819-0395, Japan.*
[c] *Department of Chemistry and Biochemistry, Kyushu University, Kyushu University, 744 Motooka, Nishi-ku, Fukuoka 819-0395, Japan.*
[d] *International Institute for Carbon Neutral Energy Research (WPI-I2CNER), Kyushu University, 744 Motooka, Nishi-ku, Fukuoka 819-0395, Japan.*
† Electronic Supplementary Information (ESI) is available. See DOI:10.1039/x0xx00000x

Molecules exhibiting TADF also seem like a natural fit for imaging and sensing because of their long-lived emission, high Φ_{PL} and good emission sensitivity to oxygen,[7] but they have only seen limited application to date. Because they can up-convert triplets excitons into singlet excitons, TADF molecules have been extensively studied as an emitter for organic light-emitting diodes (OLEDs), recently achieving high internal quantum efficiencies of nearly 100%.[8–11] Delayed emission with a long lifetime (μs to ms order) from the lowest singlet excited state (S_1) in TADF materials originates from the upconversion of a triplet in the lowest triplet excited state (T_1) to S_1 via reverse intersystem crossing (RISC) occurring at a rate that is much slower (less than 1/100) than the radiative decay from S_1. Since energy transfer from T_1 of TADF molecules to the ground state of oxygen is also much faster than RISC, the delayed fluorescence component is sensitive to oxygen. However, the charge-transfer nature of emission from most TADF molecules results in lower Φ_{PL} in highly polar solvents such as water,[12] making application of them to imaging more challenging.

Recent progress by several groups has led to TADF materials being applied in TRFM imaging as long-lived emitters. For example, Xiong et al. demonstrated TRFM imaging of cancer cells by exploiting the hydrophobic interaction between a TADF molecule and a protein.[13] Further, Zhang et al. demonstrated TRFM imaging of cancer cells by using TADF O-dots prepared with the aggregates formation by using difference of solubility,[14] and Li et al. applied TADF O-dots to in vivo TRFM imaging of zebrafish.[15] However, the Φ_{PL} values in water are still low (less than 40%) in these reports. In addition, the emission spectra often red-shifted because of the aggregation of the TADF molecules.

In this report, we demonstrate a novel preparation method to obtain TADF O-dots that are highly emissive and stable, even in water. To achieve high emissivity in water, we employed a glassy organic host matrix which can isolate the TADF emitter from high polar environment. In addition, using the host matrix avoid the dye aggregation, which red-shifts emission and

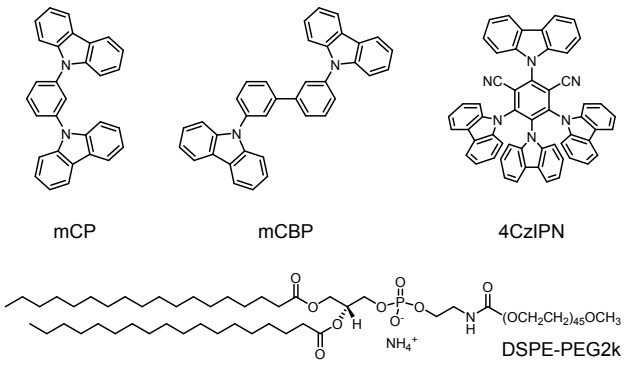

Fig. 1. Chemical structures of materials for O-dots preparation.

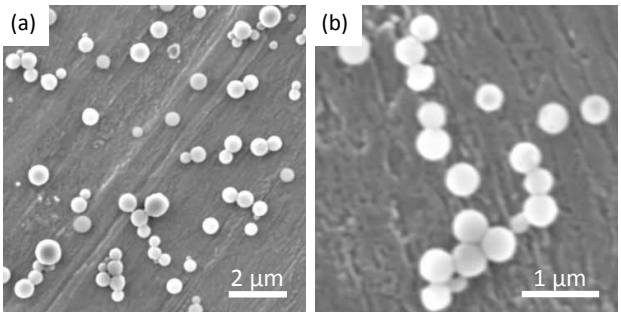

Fig. 2. SEM images of 6 wt% 4CzIPN/mCP glassy O-dots with different magnification.

decreases Φ_{PL}. To obtain the TADF material dispersed glassy state nano particle in water medium, an oil in water (o/w) emulsion was employed. For this purpose, the emitters should be dissolved into the melted host matrix homogeneously at higher temperature than melting point of the host matrices. Thus, we can get the glassy state of the solid host matrices, protecting the emitter from high polar external environment. In this case, the oxygen sensitivity of TADF materials should disappear, but the long lifetime emission should be preserved at any environments. Since the melting points of organic materials as a host matrix forming the glassy state are generally higher than the boiling point of water, we prepared O-dots under high pressure using a microwave reactor. The glassy O-dots—so named because of the glassy state of the host matrix—fabricated in this manner exhibit good stability because of protection of the emitters by the glassy host.

We chose 2,4,5,6-tetrakis(carbazol-9-yl)-1,3-dicyanobenzene (**4CzIPN**) as the TADF emitter[9,10] and used both 1,3-bis(N-carbazolyl)benzene (**mCP**) and 4,4′-bis(N-carbazolyl)-1,1′-biphenyl (**mCBP**) as host matrices (Fig. 1), because **4CzIPN**-based OLEDs exhibit excellent TADF performance with these hosts.[16,17] The energy levels of both S_1 and T_1 of **mCP** and **mCBP** (3.6 and 2.9 eV for both **mCP** and **mCBP**, respectively) are higher than those of **4CzIPN** (2.7 and 2.5 eV, respectively). Therefore, the excited energy is confined within **4CzIPN**, those result in efficient TADF emission. In addition, **mCP** and **mCBP** exhibit clear glass transitions according to differential scanning calorimetry (DSC) measurements (Fig. S1). To stabilize the dispersion of glassy O-dots in water, polyethyleneglycol (average molar weight: 2,000 Da) modified distearoyl phosphatidylethanolamine (**DSPE-PEG2k**, Fig. 1) was employed as a surfactant because of its well-known interfacial activity and biocompatibility.[18-21]

We obtained glassy O-dots according to the following procedure. From stock chloroform solutions, 0.85 mL of **mCP** solution (12.3 mmol L^{-1}), 0.3 mL of **4CzIPN** solution (1.27 mmol L^{-1}), and 0.1 mL of **DSPE-PEG2k** solution (10.6 mmol L^{-1}) were mixed in a 20 mL vial. The mixed solution was dried under the flow of nitrogen gas to obtain a thin film on the inner surface of the vial, and the film was further dried overnight under reduced pressure. After dispersing the film in 20 mL of Ar saturated water with the vortex mixing, the solution was processed in a microwave reactor (180 °C, <20 bar) for 10 min while stirring at 600 rpm. The concentrations of **mCP**, **4CzIPN**, and **DSPE-PEG2k** in water were 0.52, 0.019, and 0.053 mmol L^{-1}, respectively. After rapid cooling by blowing the vial with a stream of air, the obtained glassy O-dots were centrifuged twice at 1,500 rpm to remove the large particles. Next, the solution was centrifuged twice at 6,000 rpm to remove desorbed surfactants. Finally, we obtained 1 mL of an aqueous solution of glassy O-dots (6 wt% 4CzIPN in mCP; mCP:DSPE-PEG2k ratio is 1:1) by dispersing the precipitates to water. Henceforth, the ratio of **mCP** and **DSPE-PEG2k** are described as host/surfactant (H/S) ratio, *e.g.* H/S ratio = 10 means **mCP**:**DSPE-PEG2k** ratio is 10:1 during the preparation. The glassy O-dots either were used as prepared or were stored at −20°C as a freeze-dried powder in Ar atmosphere and then re-dispersed before use. We also prepared the neat **4CzIPN** O-dots as a reference (see ESI).[15] Recently, Zhu et al. reported neat **4CzIPN** O-dots bearing with amphiphilic peptides.[22] The photophysical properties of neat **4CzIPN** O-dots prepared by conventional method bearing with **DSPE-PEG2k** showed non-significant different with the reported values which means coated surfactant don't affected to its photophysical properties.

The obtained glassy O-dots exhibit good dispersibility over several months. Fig. 2 shows scanning electron microscope (SEM) images of glassy O-dots with **mCP** as host. The nanoparticles were spherical with diameters less than 500 nm. From dynamic light scattering (DLS) measurement with Cumulant analysis,[23] the average diameter was estimated to be 371 nm (polydispersity index was 0.093; distribution diagram was shown in Fig. S2). The DSC plot of as-prepared glassy O-dots contains a broad endothermic peak around 50–60 °C (Fig. S3). The initial and end transition temperatures of the glassy O-dots agree with the initial melting temperature of **DSPE-PEG2k** and the glass transition temperature of **mCP**. This suggests the hydrophobic part of **DSPE-PEG2k** is interacting with the hydrophobic **mCP**. Based on these results, we deduce that the glassy O-dots have a core-shell structure with a **4CzIPN**-doped core of glassy **mCP** covered with DSPE-PEG2k. On the other hand, employing **mCBP** as host resulted in the formation of microcrystals of various sizes (Fig. S4) because of the high

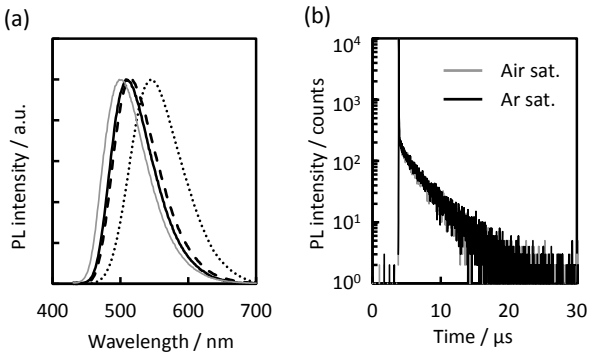

Fig. 3. (a) Emission spectra of **4CzIPN** in toluene (1.0×10^{-5} mol L^{-1}, solid grey line), **4CzIPN**/**mCP** glassy O-dots (6 wt% for H/S ratio = 1.0, solid black line), thermally evaporated **mCP** film (6 wt% doped, dashed line) and neat **4CzIPN** O-dots (dotted line). (b) Emission decay curves of 6 wt% **4CzIPN**/**mCP** glassy O-dots (prepared under O_2-free conditions) at 520 nm (λ_{ex}, 340 nm) in air or Ar saturated water.

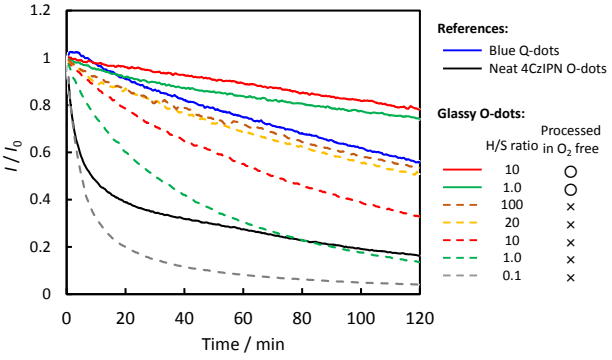

Fig. 4. Photo-degradation properties of 6wt% **4CzIPN**/**mCP** glassy O-dots with various preparation conditions, neat **4CzIPN** O-dots and blue Q-dots in water (air saturated); observed wavelength were 515, 548, 450 nm, respectively; λ_{ex}, 300–400 nm; excitation light intensity, 5 mW cm^{-2}.

melting point of **mCBP** (268.7 °C for **mCBP** compared to 178.6 °C for **mCP**). In the case of **mCBP**, the process temperature is lower than the melting point but higher than the crystallization temperature (131.3°C), leading to the crystal formation upon processing. Thus, we focused only on **mCP** as host for further experiments.

Fig. 3a shows the emission spectrum of 6 wt% **4CzIPN**/**mCP** glassy O-dots along with that of **4CzIPN** in neat O-dots prepared with conventional method,[15] in toluene, and in a 6-wt%-doped thin film of **mCP**. The emission spectrum of **mCP** was shown in Fig. S5. The emission of **4CzIPN** in 6 wt% **4CzIPN**/**mCP** glassy O-dots is similar to that in toluene and the thin film, whereas that of the neat **4CzIPN** O-dots, which do not contain **mCP**, is dramatically red-shifted. This difference in the emission spectra is the result of dispersing the emitter in a host matrix of the glassy O-dots to avoid the aggregation present in the neat **4CzIPN** O-dots. Furthermore, the glassy O-dots (H/S rate = 1.0) exhibit a higher Φ_{PL} (94%) in water compared to the neat **4CzIPN** O-dots (13%). However, fabricating the glassy O-dots in air resulted in a drastic decrease of Φ_{PL} to 64%, indicating that oxygen, which quenches **4CzIPN** triplets, is trapped in the glassy host when processed in air.

In the glassy O-dots (H/S rate = 1.0), prompt emission followed by delayed emission with a long lifetime (3.1 μs) was observed from **4CzIPN** (Fig. 3b). This delayed emission lifetime is consistent with that from the 6 wt% **4CzIPN**:**mCP** co-evaporated film (3.4 μs) and can be attributed to TADF (Fig. S6 and Table S1). On the other hand, the shorter delayed emission (1.9 μs) was observed in the neat 4CzIPN O-dots. As expected, the TADF emission from the glassy O-dots is nearly insensitive to oxygen. We attribute this to a role of the glassy host limiting the diffusion of oxygen to the emitters after formation of the glassy O-dots.

Fig. 4 shows the photo-degradation curves of glassy O-dots with different H/S ratios. Increasing the ratio of **mCP** to **DSPE-PEG2k** reduces the photo-degradation rate. Impressively, the glassy O-dots (H/S ration = 10) prepared in oxygen-free conditions achieved better photostability (LT_{50} = 360 min, Fig. S7) than the reference Q-dots having blue emission (LT_{50} = 140 min, Table S2). On the other hand, the glassy O-dots prepared in air saturated condition showed inferior stability. The preparation in oxygen-free condition might remove the oxygen in the nanoparticles and prevent the generation of reactive oxygen species inducing the photo-degradation. The good stability with high Φ_{PL} makes the TADF glassy O-dots extremely promising for use as exogenous fluorophores in bio-applications.

We tested the cell tracing properties of TADF glassy O-dots using HEK293 cells. Freeze-dried glassy O-dots (1.0 mg; H/S ratio = 10) were dispersed in 5 mL of Eagle's minimal essential medium (E-MEM). The E-MEM in a 35 mm glass-bottom dish of pre-cultured HEK293 cells (70% confluency) was replaced with E-MEM containing the glassy O-dots, and the dish was incubated for 12 h for uptake. After washing with the calcium-and-magnesium-free phosphate buffered saline (PBS(−)), the HEK293 cells were observed using phase contrast and fluorescence microscopy. Green light emission is clearly visible from the cells (Fig. 5a), and the majority of cells was not detached from the bottom of dish, indicating that the glassy O-dots have very low cytotoxicity. Given the particle size, uptake of the glassy O-dots should occur through micropinocytosis.[24] In addition, the glassy O-dots exhibit long-term cell traceability. Fig. 5b–d shows that the glassy O-dots in HEK293 cells retain their emission after 7 days of culturing through 3 passages after uptake (magnification image was shown in Fig. S8). We also checked the traceability in cells for long term. The glassy O-dots can be observed for 21 days (10 passages) (Fig. S9). The viability of HEK293 cells containing glassy O-dots was the same as control cells (Fig. S10), indicating the low cytotoxicity of the glass O-dots.

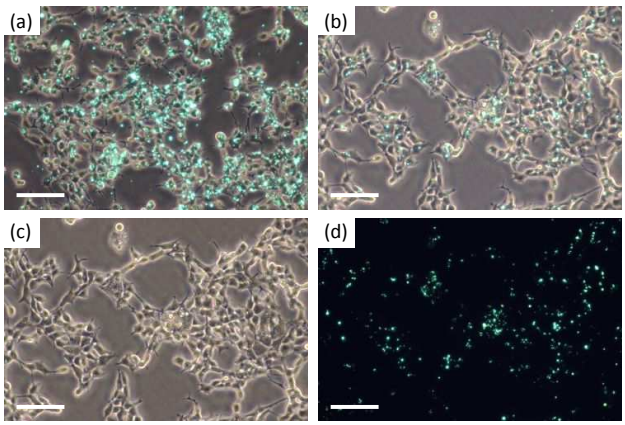

Fig. 5. Microscopic images of glassy O-dots (H/S ratio = 1.0) in HEK293 cells; (a) after uptake for 12h, (b–d) after 3 passages over 7 days following uptake; (a, b) simultaneous observation images of phase contrast and fluorescence image, (c) phase contrast image and (d) fluorescence image; scale bar, 100 μm.

We developed water-dispersible TADF glassy O-dots that exhibit very efficient (Φ_{PL} = 94%) and long-lived emission without the use of heavy metals. In addition, the TADF glassy O-dots have good photo-stability that is comparable to Q-dots. Recently, several groups have reported that O-dots based on AIEE are superior for long-term cell tracing and imaging, both in vitro and in vivo.[25-29] On the other hand, Q-dots, which are widely employed in bio-imaging, sometimes suffer from photo-bleaching and oxidative quenching by reactive oxygen species in the cells.[30-32] Therefore, glassy TADF O-dots also should be a potential application for the cell tracer and imaging, both in vitro and in vivo. In addition, the fabrication method for glassy O-dots developed here can be easily modified to produce O-dots with a wide range of properties. Several derivatives of **DSPE-PEG2k** with different reactive end groups are available commercially and could be used to enable a wide-variety of bio-applications, e.g., affinity labelling with proteins or nucleotides. Emission properties can potentially be changed by using much variety TADF materials to obtain as our request,[11] for example, deep-blue or near-infrared emission,[33,34] a narrow emission spectrum[35] and long-lived (ms order) emission.[36] Now, we are studying how to finely control the size of the glassy O-dots to further improve their suitability for use an imaging tool in bioresearch.

This research was supported by JST ERATO Grant JPMJER1305, Japan.

Notes and references

1 S. Zhang, M. Hosaka, T. Yoshihara, K. Negishi, Y. Iida, S. Tobita and T. Takeuchi, *Cancer Res.*, 2010, **70**, 4490–4498.
2 J.-C. G. Bünzli, *Chem. Rev.*, 2010, **110**, 2729–2755.
3 R. Connally, D. Veal and J. Piper, *J. Biomed. Opt.*, 2004, **9**, 725–734.
4 P. Zrazhevskiy and X. Gao, *Nat. Commun.*, 2013, **4**, 1619.
5 E. Petryayeva, W. R. Algar and I. L. Medintz, *Appl. Spec.*, 2013, **67**, 215–252.
6 J. Qian and B. Z. Tang, *Chem*, 2017, **3**, 56–91.
7 G. Méhes, H. Nomura, Q. Zhang, T. Nakagawa and C. Adachi, *Angew. Chem. Int. Ed.*, 2012, **51**, 11311–11315.
8 A. Endo, K. Sato, K. Yoshimura, T. Kai, A. Kawada, H. Miyazaki and C. Adachi, *Appl. Phys. Lett.*, 2011, **98**, 083302.
9 H. Uoyama, K. Goushi, K. Shizu, H. Nomura and C. Adachi, *Nature*, 2012, **492**, 234–238.
10 H. Kaji, H. Suzuki, T. Fukushima, K. Shizu, K. Suzuki, S. Kudo, T. Komino, H. Oiwa, F. Suzuki, A. Wakayama, Y. Murata and C. Adachi, *Nat. Commun.*, 2015, **6**, 8476.
11 M. Y. Wong and E. Zysman-Colman, *Adv. Mater.*, 2017, **29**, 1605444.
12 R. Ishimatsu, S. Matsunami, K. Shizu, C. Adachi, K. Nakano and T. Imato, *J. Phys. Chem. A.*, 2013, **117**, 5607−5612.
13 X. Xiong, F. Song, J. Wang, Y. Zhang, Y. Xue, L. Sun, N. Jiang, P. Gao, L. Tian and X. Peng, *J. Am. Chem. Soc.*, 2014, **136**, 9590−9597.
14 J. Zhang, R. Chen, Z. Zhu, C. Adachi, X. Zhang and C.-S. Lee, *ACS Appl. Mater. Interfaces*, 2015, **7**, 26266−26274.
15 T. Li, D. Yang, L. Zhai, S. Wang, B. Zhao, N. Fu, L. Wang, Y. Tao and W. Huang, *Adv. Sci.*, 2017, **4**, 1600166.
16 K. Masui, H. Nakanotani and C. Adachi, *Org. Electron.*, 2013, **14**, 2721–2726.
17 H. Nakanotani, K. Masui, J. Nishide, T. Shibata and C. Adachi, *Sci. Reports*, 2013, **3**, 2127.
18 A. Kastantin, B. Ananthanarayanan, P. Karmali, E. Ruoslahti and M. Tirrell, *Langmuir*, 2009, **25**, 7279–7286.
19 A. Priev, S. Zalipsky, R. Cohen and Y. Barenholz, *Langmuir*, 2002, **18**, 612–617.
20 B. Ashok, L. Arleth, R. P. Hjelm, I. Rubinstein and H. Önyüksel, *J. Pharm. Sci.*, 2004, **93**, 2476–2487.
21 R. Wang, R. Xiao, Z. Zheng, L. Xu and J. Wang, *Int. J. Nanomed.*, 2012, **7**, 4185–4198.
22 Z. Zhu, D. Tian, P. Gao, K. Wang, Y. Li, X. Shu, J. Zhu and Q. Zhao, *J. Am, Chem. Soc.*, 2018, **140**, 17484–17491.
23 D. E. Koppel, *J. Chem. Phys.*, 1972, **57**, 4814–4820.
24 J. P. Lim and P. A. Gleeson, Immunol. *Cell Biol.*, 2011, **89**, 836–843.
25 Y. Yu, C. Feng, Y. Hong, J. Liu, S. Chen, K. M. Ng, K. Q. Luo and B. Z. Tang, *Adv. Mater.*, 2011, **23**, 3298–3302.
26 K. Li, W. Qin, D. Ding, N. Tomczak, J. Geng, R. Liu, J. Liu, X. Zhang, H. Liu, B. Liu and B. Z. Tang, *Sci. Reports*, 2013, **3**, 1150.
27 Z. Wang, S. Chen, J. W. Y. Lam, W. Qin, R. T. K. Kwok, N. Xie, Q. Hu and B. Z. Tang, *J. Am. Chem. Soc.*, 2013, **135**, 8238–8245.
28 Z. Wang, T.-Y. Yong, J. Wan, Z.-H. Li, H. Zhao, Y. Zhao, L. Gan, X.-L. Yang, H.-B. Xu and C. Zhang, *ACS Appl. Mater. Interfaces*, 2015, **7**, 3420–3425.
29 Z. Wang, L. Yang, Y. Liu, X. Huang, F. Qiao, W. Qin, Q. Hu and B. Z. Tang, *J. Mater. Chem. B*, 2017, **5**, 4981–4987.
30 M. C. Mancini, B. A. Kairdolf, A. M. Smith and S. Nie, *J. Am. Chem. Soc.*, 2008, **130**, 10836–10837.
31 Y. Wang and M. Tang, *Sci. Tot. Environ.*, 2013, **625**, 940–962.
32 S. J. Soenen, S. Abe, B. B. Manshian,T. Aubert, Z. Hens,S. C. De Smedt and K. Braeckmans, *J. Biomed. Nanotechnol.*, 2015, **11**, 631–643.
33 L.-S. Cui, H. Nomura, Y. Geng, J. U. Kim, H. Nakanotani, C. Adachi, *Angew. Chem. Int. Ed.*, 2017, **56**, 1571‑1575.
34 T. Yamanaka, H. Nakanotani, S. Hara, T. Hirohata and C. Adachi, *Appl. Phys. Express*, 2017, **10**, 074101.
35 T. Hatakeyama, K. Shiren, K. Nakajima, S. Nomura, S. Nakatsuka, K. Kinoshita, J. Ni, Y. Ono, T. Ikuta, 2016, **28**, 2777-2781.
36 H. Noda, H. Nakanotani, C. Adachi, Chem. Lett., 2019, **48**, 126–129.